Nat. Hazards Earth Syst. Sci. Discuss., 1, 3577–3624, 2013
www.nat-hazards-earth-syst-sci-discuss.net/1/3577/2013/
doi:10.5194/nhessd-1-3577-2013

Natural Hazards and Earth System Sciences
Open Access
Discussions

Fully integrated physically-based numerical modelling of impacts of groundwater extraction on surface and irrigation-induced groundwater interactions: case study Lower River Murray, Australia

S. Alaghmand[1], **S. Beecham**[1], **and A. Hassanli**[1,2]

[1]Centre for Water Management and Reuse, School of Natural and Built Environments, University of South Australia, Adelaide, Australia
[2]College of Agriculture, Shiraz University, Shiraz, Iran

Received: 24 April 2013 – Accepted: 6 July 2013 – Published: 26 July 2013

Correspondence to: S. Alaghmand (sina.alaghmand@mymail.unisa.edu.au)

Published by Copernicus Publications on behalf of the European Geosciences Union.

Abstract

Combination of reduction in the frequency, duration and magnitude of natural floods, rising saline water-table in floodplains and excessive evapotranspiration have led to an irrigation-induced groundwater mound forced the naturally saline groundwater onto the floodplain in the Lower River Murray. It is during the attenuation phase of floods that these large salt accumulations are likely to be mobilised and will discharge into the river. The Independent Audit Group for Salinity highlighted this as the most significant risk in the Murray–Darling Basin. South Australian government and catchment management authorities have developed salt interception schemes (SIS). This is to pump the highly saline groundwater from the floodplain aquifer to evaporation basins in order to reduce the hydraulic gradient that drives the regional saline groundwater towards the River Murray. This paper investigates the interactions between a river (River Murray in South Australia) and a saline semi-arid floodplain (Clarks Floodplain) significantly influenced by groundwater lowering (Bookpurnong SIS). Results confirm that groundwater extraction maintain a lower water-table and more fresh river water flux to the saline floodplain aquifer. In term of salinity, this may lead to less amount of solute stored in the floodplain aquifer. This occurs through two mechanisms; extracting some of the solute mass from the system and changing the floodplain groundwater regime from a losing to gaining one. Finally, it is shown that groundwater extraction is able to remove some amount of solute stored in the unsaturated zone and mitigate the floodplain salinity risk.

1 Introduction

As groundwater moves from highland aquifer to the river, it needs to pass under the floodplain. Due to high rate of evapotranspiration in arid and semi-arid regions, such as Lower Murray River in South Australia, part of groundwater discharges to the floodplain and leaves salt in the floodplain soil (Fig. 1). Overbank floods leach salt to the groundwater, wash salt off the salt and add water to the floodplain soils. The highly variable

NHESSD
1, 3577–3624, 2013

nature of surface flow in arid/semi-arid regions has led to regulation of rivers by weirs and storages instructions (Jolly et al., 1996) which has affected surface-groundwater interactions in the floodplains for instance, the removal of salt by overbank floods occurs less frequently. A combination of reduction in the frequency, duration and magnitude of natural floods, rising saline water-table in floodplains (due to river manipulations and irrigated agricultural land drainage) and excessive evapotranspiration (ET) have led to an irrigation-induced groundwater mound forced the naturally saline groundwater onto the floodplain at a relatively high flow rate (Jolly et al., 1993; Holland et al., 2009a). This has caused reduction of leaching of salt from root zones and accumulation of salt in unsaturated zones causing dieback of environmentally important riparian vegetation such as red gum (*Eucalyptus camaldulensis*) and black box (*Eucalytpus largiflorens*) and a decline in river water quality (Allison, 1990; Herczeg, 1993; Jolly et al., 1993, 1996; Peck and Hurle, 1973; Peck and Hatton, 2003). Another example is Mona Park district along the Burdekin River in Northern Australia. Wide spread use and application of "imported" surface water has resulted in rising water-table levels. Particular concern arose for the after a large groundwater mound formed during the wet season of 2000 (Petheram et al., 2008).

Until 2011 there has not been a high river flood event for past 13 yr but salt has been accumulating in the floodplain during this period. The sediments underlying irrigation areas have also been inducing salt problems. It is during the attenuation phase of floods that these large salt accumulations are likely to be mobilised and will discharge into the river. The Independent Audit Group for Salinity (IAG-Salinity) in their report (MDBA, 2010) mentioned the likelihood of severe salt accessions during flood recessions. This was articulated in their Recommendation 1 and in the previous audit reports. The IAG-Salinity considers this as the most significant risk in the Murray–Darling Basin. As an effort to reduce the immediate risk of river salt accession induced by increased saline groundwater levels, due to field irrigation and excessive evaporation, there has been significant investment into the design and construction of salt interception schemes (SISs) along the River Murray. South Australian government and

NHESSD
1, 3577–3624, 2013

catchment management authorities have developed salt interception schemes to pump the highly saline groundwater mixed with irrigation recharge from the floodplain to evaporation basins (DWR, 2001). The Bookpurnong floodplain salt interception scheme (SIS) was constructed in 2005, with seven highland and 16 floodplain groundwater production pumping bores, including six bores on the Bookpurnong floodplain. Each bore yields 2–3 $L s^{-1}$ to reduce the hydraulic gradient that drives the regional saline groundwater towards the River Murray and improve river water quality (Berens et al., 2009). The SIS bores have been in operational since August 2005 except some periods that was shut down (e.g. from November 2006 to May 2007). It is expected they will prevent about 200 tonnes of salt per day from entering the River Murray by 2040 (White et al., 2009). Before the SISs were operational, an irrigation-induced groundwater mound forced the naturally saline groundwater onto the floodplain at a relatively high flow rate, thereby increasing soil salinity in the root zone of the floodplain woodlands (Viezzoli et al., 2009; Doble, 2004) (Fig. 1). Clarks Floodplain has been targeted as a test site to determine the benefits of salt interception. As field investigations have shown that significant salt accumulation and vegetation dieback has occurred due to increased irrigation in the surrounding highlands at this floodplain (Doble, 2004).

Some of the most challenging aspects of water resources studies concern the interaction between surface and groundwater (Wheater et al., 2010). Rassam (2011) summarized flow and solute exchange between a river and a floodplain aquifer into four categories: (1) natural exchange flux due to river stage fluctuations such as flooding (within-bank or overbank), base-flow discharge, reservoir regulations, etc. (Squillace, 1996; Chen, 2003; Moench and Barlow, 2000; Brutsaert and Lopez, 1998), (2) exchange flux induced by pumping wells in the adjacent aquifers (Chen and Shu, 2006; Sophocleous et al., 1995; Sun and Zhan, 2007), (3) exchange flux due to change in recharge rate; and (4) exchange flux due to changes in evapotranspiration. Groundwater extraction is one of the most important processes that impact the exchange flux between surface and groundwater water. Extraction-induced river depletion is defined as the reduction of river flow due to induced infiltration of stream water into the aquifer

NHESSD
1, 3577–3624, 2013

or the capture of aquifer discharge to the river (Rassam, 2011). The temporal and spatial scales at which these processes contribute to the exchange flux is variable. For instance, river depletion resulting from groundwater extraction is delayed by time lags that range from days to hundreds of years; the extent of the extraction activity may vary along a river reach thus leading to gaining and losing sub-reaches. Because of the intensive spatial and temporal variability there is a need for dynamic modelling of their impacts on river flow.

Near-river-aquifer systems are complex due to the difficulties in estimating flows and solute mass into and out of the aquifer, the complicated nature of the GW-SW interaction processes, and the uncertainty of aquifer properties (Sophocleous, 2010). Because of this complexity, computer models are used to model groundwater systems and estimate the exchange flux between surface water and ground-water. These models are computer-based numerical solutions to the boundary value problems of concern (Wheater et al., 2010). In this regard, the need to accurately quantify and forecast surface and groundwater interactions has promoted the use of physically-based numerical modelling approaches in many studies (Loague and VanderKwaak, 2004; Ebel and Loague, 2006; Beven and Binley, 1992; Beven, 2006, 2002, 2001; Nasonova and Gusev, 2008). Physically-based models are generally founded on the blueprint for a physically-based mathematical model of a complete hydrological system developed by Freeze and Harlan (1969). Popular physically-based models include HydroGeoSphere (HGS) (Therrien et al., 2005), Integrated Hydrology Model (InHM) (VanderKwaak and Loague, 2001; VanderKwaak, 1999), MODular Hydrologic Modelling System (MODHMS) (HydroGeoLogic Inc, 2006), ParFlow (Kollet and Maxwell, 2006), MIKE SHE (Abbott et al., 1986), Modular Modelling System (MMS) (Leavesley et al., 1996), CATchmentHYdrology (CATHY) (Camporese et al., 2010), FIPR hydrologic model (FHM) (Ross et al., 1997), and Penn State Integrated Hydrologic Model (PIHM) (Qu and Duffy, 2007). Modelling of surface-groundwater interaction needs knowledge of groundwater modelling, but also a detailed understanding of the exchange processes that occur between the surface and sub-surface domains (Barnett

NHESSD
1, 3577–3624, 2013

et al., 2012). Surface-groundwater interactions have been investigated in several studies (Hoehn and Scholtis, 2011; Lenahan and Bristow, 2010; Sophocleous and Perkins, 2000; Winter, 1999; Kollet and Maxwell, 2006; Krause et al., 2007; Lamontagne et al., 2005; Liang et al., 2007; Meire et al., 2010; Panday and Huyakorn, 2004; Shlychkov, 2008), but floodplains in arid/semi-arid regions have received considerably little attention (Jolly et al., 2008). One of the major limitation in this regard is lack of high quality observed data (Pilgrim et al., 1988). This has resulted in application of experiences from humid regions in drier regions without knowledge of the consequences. At best, such results will be highly inaccurate while at worst, they can be the adopted for inappropriate management solutions which disregards the features of arid/semi-arid areas (Wheater et al., 2010). One issue can be the key role of salinity in arid and semi-arid floodplains (Hart et al., 1991) and role of the unsaturated zone as one of the main compartments of solute mass storage in the system.

This paper investigates the interactions between a river (River Murray in South Australia) and a saline floodplain (Clarks Floodplain) in asemi-arid area significantly influenced by groundwater lowering (Bookpurnong SIS). Hence, the main objective of this research is to quantify the relative impacts of the groundwater lowering on the surface-groundwater interactions in semi-arid saline floodplain highlighting the dynamics of flow and solute. To this aim two numerical model scenarios are defined including the one withSIS operation (with-SIS) and another one without SIS operation (without-SIS). The question is what could be the water and solute dynamic at the study site if there was not any groundwater lowering. It was hypothesized that groundwater extraction via SIS may lead to lower water-table and less saline floodplain aquifer. Moreover, the HGSs capabilities to reproduce surface and groundwater flow and solute dynamics are also tested. In this regard, HGS model is developed and calibrated according to well-documented observed surface and groundwater data. This paper comprises of two sections; developing and calibrating the numerical model and applying the model according to the defined scenarios. During evaluating the scenarios the calibrated model (2006–2010) is used without further parameters changes.

NHESSD
1, 3577–3624, 2013

2 Study site

The study was conducted over the Clarks floodplain adjacent to the Murray River in the Bookpurnong Irrigation District of the Riverland region of South Australia (Fig. 2). The area, located ~ 12 km upstream from the township of Loxton, has been the focus of trials to manage a marked decline in tree health that has been observed along the River Murray in South Australia. The study site is typically vegetated by a mixture of river red gum (*Eucalyptus camaldulensis*), black box (*Eucalyptus largiflorens*), river cooba (*Acacia stenophylla*) and lignum (*Muehlenbeckia florenta*). The study site is located within the semi-arid inland of Australia, with annual rainfall varying between 200 and 300 mm and annual potentialevaporation of approximately 1800 mm.

The Coonambidgal Clay ranges from 2 to 7 m thick, while the Monoman Formation is approximately 7 m thick in this area. The cliffs adjacent the floodplains consist of a layer of Woorinen Sands over Blanchtown Clay, each approximately 2 m thick, overlying a layer of Loxton Sands up to 35 m in depth. The whole area is underlain by the Bookpurnong Beds, which act as an aquitard basement to the shallow aquifer that encompasses the Monoman Formation and Loxton Sands (Doble et al., 2006). The Bookpurnong Beds act as an aquitard basement to the shallow, unconfined aquifer that encompasses the Monoman Formation and Loxton Sands. Saline groundwater lies beneath the floodplain, within the Monoman Formation, with the depth to water-table ranging from 2 to 4 m below the surface. The majority of the floodplain groundwater has an approximate conductivity of 50 000 ($\mu S\,cm^{-1}$). It is worth noting that the physiological limit for water uptake in this environment is 30 000 ($\mu S\,cm^{-1}$) by river red gums and 55 000 ($\mu S\,cm^{-1}$) by black box trees (Overton and Jolly, 2004). More detailed description of the study site is discussed by Brown and Stephenson (1991), Jarwal et al. (1996) and Doble et al. (2006).

NHESSD
1, 3577–3624, 2013

3 Numerical model

The HydroGeoSphere (HGS) model provides a rigorous simulation capability that combines fully-integrated hydrologic/water quality/subsurface and transport capabilities with a well-tested set of user interface tools. The subsurface module is based on the University of Waterloo and Université Laval three-dimensional (3-D) subsurface and transport code FRAC3DVS (Therrien, 1992). The surface module is based on the Surface Water Flow Package of the MODHMS simulator, which is itself an enhancement of the popular US Geological Survey code MODFLOW (Brunner and Simmons, 2012). The numerical formulation of HGS is based on the assumption that a subsurface flow equation for a porous saturated or unsaturated medium is always solved. A 3-D modified formulation of the Richards equation is applied. The van Genuchten (1980) or Brooks–Corey (Brooks and Corey, 1964) relationships are available to relate pressure head to saturation and relative hydraulic conductivity. Surface water flow is simulated using a 2-D depth-averaged flow equation (the diffusion-wave approximation of the Saint–Venant equations). The common node approach (based on conductivity of hydraulic head between two domains) (Therrien and Sudicky, 1996) and dual node approach (based on a first-order exchange coefficient) are used in HGS in order to couple surface and subsurface media. HGS requires pre- and post-processor tools in order to handle input preparation (complex topography and grid) and visualization of the outputs. In this study, Grid Builder (McLaren, 2005) and Groundwater Modelling system (GMS) (AquaVeo, 2011) are used as pre-processors to generate the input grid domain. Also, GMS was applied as a post-processor to visualize the model results. The next section describes the governing equations of the model.

3.1 Governing equations

The following text derived from Therrien et al. (2010b). The HGS uses the following modified form of Richards' equation to describe three-dimensional transient subsurface

NHESSD
1, 3577–3624, 2013

flow in a variably-saturated porous medium:

$$-\nabla \cdot (w_m q) + \sum \Gamma ex \pm Q = w_m \frac{\partial}{\partial t}(\theta_s S_w) \quad (1)$$

where w_m [dimensionless] is the volumetric fraction of the total porosity occupied by the porous medium (or primary continuum). The fluid flux q [LT^{-1}] is given by:

$$q = -K \cdot k_r \nabla(\psi + z) \quad (2)$$

where $k_r = k_r(S_w)$ represents the relative permeability of the medium [dimensionless] with respect to the degree of water saturation S_w [dimensionless], ψ is the pressure head [L], z is the elevation head [L] and θ_s is the saturated water content which is assumed equal to the porosity. Fluid exchange with the outside of the simulation domain, as specified from boundary conditions, is represented by Q which is a volumetric fluid flux per unit volume representing a source (positive) or a sink (negative) to the porous medium system.

The hydraulic conductivity tensor, K [LT^{-1}], is given by:

$$K = \frac{\rho g}{\mu} k \quad (3)$$

where where g is the gravitational acceleration [LT^{-2}], μ is the viscosity of water [$M L^{-1} T^{-1}$], k is the permeability tensor of the porous medium [L^2] and ρ is the density of water [ML^{-3}], which can be a function of the concentration C [$M L^{-3}$] of any given solute such that $\rho = \rho(C)$.

Water saturation is related to the water content θ [dimensionless] according to:

$$S_w = \frac{\theta}{\theta_s} \quad (4)$$

The two-dimensional Saint Venant equations for unsteady shallow water flow consist of 3 equations, which are given by the following mass balance equation:

$$\frac{\partial \phi_0 h_0}{\partial t} + \frac{\partial (\upsilon_{x0} d_0)}{\partial x} + \frac{\partial (\upsilon_{y0} d_0)}{\partial y} + d_0 \Gamma_0 \pm Q_0 = 0 \quad (5)$$

NHESSD
1, 3577–3624, 2013

coupled with the momentum equation for the x direction:

$$\frac{\partial}{\partial t}(\upsilon_{x0} d_0) + \frac{\partial}{\partial x}\left(\upsilon_{x0}^2 d_0\right) + \frac{\partial}{\partial y}(\upsilon_{x0}\upsilon_{y0} d_0) + g d_0 \frac{\partial d_0}{\partial x} = g d_0 (S_{ox} - S_{fx}) \quad (6)$$

and the momentum equation for the y direction:

$$\frac{\partial}{\partial t}(\upsilon_{y0} d_0) + \frac{\partial}{\partial y}(\upsilon_{y0} d_0) + \frac{\partial}{\partial x}(\upsilon_{x0}\upsilon_{y0} d_0) + g d_0 \frac{\partial d_0}{\partial x} = g d_0 (S_{oy} - S_{fy}) \quad (7)$$

where d_0 is the depth of flow [L], z_0 is the bed (land surface) elevation [L], h_0 is thewater surface elevation [L], υ_{x0} and υ_{y0} are the vertically averaged flow velocities in the x and y directions [$\mathrm{L\,T^{-1}}$], Q_0 is a volumetric flow rate per unit area representing external source and sinks [$\mathrm{L\,T^{-1}}$], and ϕ_0 is a surface flow domain porosity which is unity for flow over a flat plane, and varies between zero at the land surface and unity at the top of all rills and obstructions, for flow over an uneven surface.

Three-dimensional transport of solutes in a variably-saturated porous matrix is described by the following equation:

$$-\nabla \cdot w_m (qC - \theta_s S_w D \nabla C) + [w_m \theta_s S_w R \lambda C] + \sum \Omega_{ex} \pm Q_c = w_m \left[\frac{\partial(\theta_s S_w R \lambda C)}{\partial t} + \theta_s S_w R \lambda C\right] \quad (8)$$

where C is the solute concentration [$\mathrm{M\,L^{-3}}$] of the current species amongst possibly multiple species and λ is a first-order decay constant [$\mathrm{L^{-1}}$]. Solute exchange with the outside of the simulation domain, as specified from boundary conditions, is represented by Q_c [$\mathrm{M\,L^{-3}\,T^{-1}}$] which represents a source (positive) or a sink (negative) to the porous medium system. The dimensionless retardation factor, R, is given by:

$$R = 1 + \frac{\rho_b}{\theta_s S_w} K' \quad (9)$$

where ρ_b is the bulk density of the porous medium [$\mathrm{M\,L^{-3}}$] and K' is the equilibrium distribution coeffiient describing a linear Freundlich adsorption isotherm [$\mathrm{L^{-3}\,M}$].

NHESSD
1, 3577–3624, 2013

The hydrodynamic dispersion tensor D [$L^2 T^{-1}$] is given by:

$$\theta_s S_w D = (\alpha_l - \alpha_t)\frac{qq}{q} + \alpha_t q I + \theta_s S_w \tau D_{free} I \quad (10)$$

where α_l and α_t are the longitudinal and transverse dispersivities [L], respectively, q is the magnitude of the Darcy flux, τ is the matrix tortuosity [dimensionless], D_{free} is the free-solution diffiusion efficient [$L^2 T^{-1}$] and I is the identity tensor. The product τD_{free} represents an effective diffusion coefficient for the matrix.

ET is calculated as a combination of transpiration and evaporation. Transpiration from vegetation occurs within the root zone of the subsurface and is a function of the leaf area index (LAI) [dimensionless], nodal water (moisture) content (θ) [dimensionless] and a root distribution function (RDF) over a prescribed extinction depth. The rate of transpiration (Tp) is estimated using the following relationships (Kristensen and Jensen, 1975):

$$\mathrm{Tp} = f1(\mathrm{LAI})\, f2(\theta)\, \mathrm{RDF}[\mathrm{Ep} - \mathrm{Ecan}] \quad (11)$$

where Ep is the reference potential evapotranspiration which may be derived from pan measurements or computed from vegetation and climatic factors [$L T^{-1}$] and Ecan is the tree canopy evaporation [$L T^{-1}$]. The value and description of Ep has followed the notation and conceptualization of Therrien et al. (2010a) and Kristensen and Jensen (1975). The vegetation function ($f1$) correlates the transpiration (Tp) with the leaf area index (LAI) in a linear fashion and the moisture content (θ) function ($f2$) correlates Tp with the moisture state at the roots. The root zone distribution function (RDF) is defined by the relationship:

$$\mathrm{RDF} = \frac{\int_{c1}^{c2} \mathrm{rF}(z)\,\mathrm{d}z}{\int_0^{L_r} \mathrm{rF}(z)\,\mathrm{d}z} \quad (12)$$

where C1 and C2 are dimensionless fitting parameters, Lris the effective root length [L], z is the depth coordinate from the soil surface [L] and rF(z) is the root extraction

NHESSD
1, 3577–3624, 2013

function [L^3T^{-1}] which typically varies logarithmically with depth. Below the wilting point moisture content, transpiration is 0; transpiration then increases to a maximum at the field capacity moisture content. This maximum is maintained up to the oxic moisture content, beyond which the transpiration decreases to 0 at the anoxic moisture content. When available moisture is larger than the anoxic moisture content, the roots become inactive due to lack of aeration (Therrien et al., 2010a).

In HGS, evaporation from the soil surface and subsurface soil layers is a function of nodal water content and an evaporation distribution function (EDF) over a prescribed extinction depth. The model assumes that evaporation (Es) occurs along with transpiration, resulting from energy that penetrates the vegetation cover and is expressed as (Therrien et al., 2010a):

$$Es = \alpha \cdot (Ep - Ecan)[1 - f1(LAI)x]EDF \quad (13)$$

Where α is a wetness factor which depends on the moisture content at the end of the energy-limiting stage and below which evaporation is 0. For further details on the code the reader is referred to Therrien et al. (2010a).

3.2 Model set-up

The River Murray 2008 Stitched Digital Elevation Model (DEM) was one of several outputs delivered through the Imagery Baseline Data Program, completed late 2008 by Department for Water, Government of South Australia. The DEM, completed by CSIRO, is a product of several smaller "River Murray" DEMs, stitched together using GIS methods. The resolution of these DEMs ranged from 2 m to 50 m with the final stitched DEM having a resolution of 2 m. Where LiDAR has been used to acquire data, the vertical accuracy is approximately ±0.15–0.2 m. For this study, the Digital Elevation Model (DEM) of the study site was generated at 10 m grid resolution using LiDAR data. 10 m grid resolution seemed to be an optimal resolution as finer resolution made the model too large to be modelled. Still, 10 m grid resolution is able to represent the study area efficiently.

NHESSD
1, 3577–3624, 2013

A total of 20 sub-layers were considered including finer grids, 15 sub-layers for the top 5 m, and relatively larger for lower layers, 5 sub-layers for buttom10 m. The final geometry grid consists of 78 624 nodes that form 143 500 elements. As illustrated in Fig. 3, the geometry grid covers part of Clark's floodplain from the floodplain slope break to the River Murray main channel. This includes two SIS production wells (32FP and 34FP) and nine observation wells. In this case, the length of the river bank was 570 m and the distance from the river bank to the SIS well varies between 480 m and 650 m. Two types of soil layers are constructed according to drill log data. The 10 m thick Monoman Formation Sand is overlaid by spatially variable semi-confining heavy Coonambidgal Clay (Fig. 3).

The properties of the porous media (soil) of the model and unsaturated van Genuchten function parameters (van Genuchten, 1980) are adopted from Jolly et al. (1993) and Doble et al. (2006) who adjusted and proposed van Genuchten functions parameters for the Lower Murray River soil types including semi-confining heavy Coonambidgal Clay, Monoman Sand and two forms of the transition layer (Table 1). In natural condition, the hydraulic parameters of the surface domain (river bed and floodplain corridor) have significant differences and so divided in the model into main channel (river) and floodplain. Table 2 indicates the values used as surface properties of the numerical model (Therrien et al., 2005). During the time frame of the model no flow above the river bank has occurred (i.e. only non-flooding conditions occurred) and so the surface properties of the floodplain are not that sensitive in the model.

ET is one of the main drivers of the hydrological processes in an arid/semi-arid region, such as the lower River Murray (Doble et al., 2006; Holland et al., 2009a). The two main vegetation types occurring at the study site (Eucalyptus tree and grass) have significantly different characteristics in terms of root depth, water demand and leaf area index. In order to obtain a better representation of the actual condition, vegetation coverage of the floodplain was customized into two different categories. Normalized evaporation and root depth functions are mapped onto porous media elements above the maximum depths. Currently, four evaporation and root depth functions are available in

NHESSD
1, 3577–3624, 2013

HGS; constant, linear, quadratic and cubic. In this study, quadratic evaporation and root depth functions are applied. Table 3 shows the values of ET components for Eucalyptus and grass adopted from Hingston et al. (1997), Banks et al. (2011), and Verstrepen (2011).

The boundary conditions for the numerical model of the study site includespecified heads for the porous media domain at the end of the floodplain of the model. In this case, observed groundwater heads at the location of the 31FO, 33FO and 35FO are assigned to the nodes along the model edge as shown in Fig. 3. On the other hand, groundwater lowering through production wells was represented by lowering the head at the location of the 32FP and 34FP consistence with their recorded pumping rates. Observed river levels for the surface domain were set at the river side of the model. In this regard, the observed water levels downstream of Lock 4 were applied to the river nodes of the model. In addition, rainfall was simulated for the entire model surface domain beginning on day 1. Other aerial boundary condition was assigned in the ET domain. ET was dynamically simulated as a combination of evaporation and transpiration processes by removing water from all model cells of the surface and subsurface flow domains within the defined zone of the evaporation and root extinction depths. The daily rainfall and potential evaporation values used in the model were based on the recorded daily rainfall at the Loxton station. Figure 3 illustrates the configuration of all boundary conditions of the model.

Initial conditions refer to the head and solute concentration distributions everywhere in the model at the beginning of the simulation. In this context, field-measured head values or solute concentrations do not represent the real initial condition as they are obtained at a time when the natural ground-water system is in equilibrium (Barnett et al., 2012). For instance, if the field-observed data values are used as initial conditions, the model response in the early time steps would reflect not only the model stress under study but also the adjustment of model head values to offset the lack of correspondence between model hydrologic inputs and parameters and the initial head values (Franke et al., 1987). Therefore, in a transient state problem, the initial

NHESSD
1, 3577–3624, 2013

conditions should be determined through a steady/dynamic steady-state solution to generate dynamic cyclic initial conditions such as evaporation and rainfall seasonal cycles (Anderson and Woessner, 1992). Barnett et al. (2012) suggested carrying out a simulation which begins long enough before the calibration period allowing for an initial model equilibration time. In this study, stress period starts from 1 January 2006 and ends on 1 September 2010. So, the initial model covers 30 yr to create the equilibrium initial condition for the stress period. The initial model was intended to show equilibrium behaviour while its last time steps should be equal to the first time steps of the stress model which are observed (Fig. 4). Hence, simulated GW heads are compared with absolute observed values at observation wells (BO1: 10.4, B2O: 10.15, BO3: 10.01, BO4: 10.20, BO5: 10.14 and BO6: 10.07 mAHD, Holland et al., 2009c). Also, the status of the solute concentration distribution at the beginning of the study (stress) period was checked with the general solute distribution pattern at the floodplain which was observed in the field and the related reports. This can be considered as two zones; relatively fresh GW zone within 50 m distance of the river banks (BO1: 6500 $\mu S\,cm^{-1}$ and BO4: 1200 $\mu S\,cm^{-1}$) and saline zone (BO2: 53 000 $\mu S\,cm^{-1}$, BO3: 54 000 $\mu S\,cm^{-1}$, BO5: 50 900 $\mu S\,cm^{-1}$and BO6: 52 000 $\mu S\,cm^{-1}$) for the rest of the floodplain (Holland et al., 2009c).

3.3 Coupled flow and transport calibration

Observed hydraulic heads and groundwater solute concentrations at the observation wells are used as calibration criteria during coupled flow-and-transport calibration of the model (Barnett et al., 2012). This process aims to assess the ability of the surface-groundwater model to correctly distribute water and solute between the two domains (Li et al., 2008). Two different approaches are employed for the flow and solute calibrations. While, the aim of the calibration process for groundwater flow was to match the absolute observed hydraulic heads at the observation wells, given the difficulty associated with the quantification of the solute transport model parameters (lack of accurate estimations of the hydraulic conductivity and porosity of the aquifer, etc.), the solute

NHESSD
1, 3577–3624, 2013

was calibrated to the observed concentration patterns. This was because concentration patterns are much more sensitive to local-scale geological heterogeneity than are hydraulic heads, and models may have difficulty reproducing the concentrations or their temporal variability at single observation wells. Hence, in this case, because of significant salinity differences between 50 m distance to the river bank (BO1 and BO4: EC < 7000 $\mu S\,cm^{-1}$) and the rest of the floodplain (BO2, BO3, BO5 and BO6: EC = 30 000–50 000 $\mu S\,cm^{-1}$), an aggregate quantity like the plume mass is a more suitable calibration criterion (Barnett et al., 2012).

Calibration of the model was conducted manually with more consideration to the sensitive parameters. The model performance for both flow and solute transport was tested by visual comparison between observed and simulated series of hydraulic heads and solute concentrations at observation wells BO1, BO2, BO3, BO4, BO5 and BO6. Moreover, quantitative evaluation was undertaken using goodness-of-fit measures. Figure 5 demonstrates the performance of the calibrated model of the Clarks Floodplain. Seeking to minimise a measure of goodness of fit during the calibration period, or to achieve a specific predefined value of goodness of fit, may be the best way to increase confidence in predictions (Barnett et al., 2012). The goodness-of-fit measures, including root *r*-square (R^2), Nash–Sutcliffe (*Nr*), mean sum of residuals (MSR) and root mean squared error (RMSE), are used to evaluate the simulated values against the observed data (Table 4). Moreover, the solute concentration distribution results show that the calibrated model was able to reproduce the surface-groundwater interaction processes in an acceptable manner as they present a good agreement. For instance, the EM31 survey in November 2007 showed a distinct zone of low conductivity along the eastern margin abutting the river channel. This shows the presence of freshwater within the floodplain aquifer (bank storage) and was supported by groundwater salinity data collected at the riverbank piezometers at that time. Figure 6 visualizes the snapshot of the solute distribution for the calibration model at last day of the simulation (1 September 2010).

NHESSD
1, 3577–3624, 2013

4 Results and discussions

Often the objectives of numerical modelling involve a quantitative assessment of the response of heads or solute concentrations to future stresses on the surface or subsurface system. Predictive scenarios can be formulated to quantify groundwater behaviour in either absolute or relative terms. In the case of the latter, the particular modelling outcome is obtained by subtracting one model result from another (null scenario). A null scenario is a predictive model that has no future changes in the stresses that are being investigated. Considering the prediction approach suggested in the Australian groundwater modelling guidelines (Barnett et al., 2012), even though it may be difficult to calibrate the surface–groundwater interaction model, at the same time there may be reasonable confidence in a model to predict the right trends. In these situations, it is not common practice for one set of predictions to be made using the best possible model, and for further predictions to be presented in absolute terms. Rather, the differences are often presented relative to this base case. In this case, to investigate the surface-groundwater interactionsinduced by groundwater lowering, the calibrated model (2006–2010) was used as the null scenario without further parameter changes to investigate the water balance and the solute mass balance. It should be cautioned that results discussed here are based on a calibrated numerical model based on available data that may include some uncertainties particularly in term of solute dynamics. Figure 7 shows the groundwater heads at the boundary of the models (SIS wells) for the defined scenarios. In without-SIS scenario there are constant values equal to 10.1 m for 31FO, 10.25 m for 33FO and 10.01 m for 35FO (observed just before commencement of the SIS production wells). This assumes no significant groundwater head changes were occurred. For the with-SIS scenario it is influenced by SIS production wells.

4.1 Water balance

One of the main starting points for analysis of the flow dynamics in a surface-groundwater system is accurate modelling of the water balance. In this case, three

NHESSD
1, 3577–3624, 2013

forms of water balance outputs are considered as indicators to compare the scenarios. These indicators include changes in water storage in the porous and/or overland domain, the amount of water movement between the two domains (flow flux) and the groundwater head profile along the observation transects. Hence, three outputs of the model are considered in the analysis of the system water balance of including the accumulation rate in the porous medium ($m^3\,day^{-1}$), flux (m^3) from the river to the floodplain aquifer and groundwater head profile alongtransectB1.

The accumulation rate represents the changes in water storage that occurs in the floodplain aquifer. As shown in Fig. 8, the water accumulation ratefor the without-SIS scenario shows a relative balanced trend during the study period. A correlation between the accumulation rate and the river water level fluctuation are observed. This is because asthe river water level increases, the accumulation rate increases as more surface water is stored in the floodplain aquifer. In contrast, a river water level decrease leads to a lower accumulation rate. Note that in this study a constant groundwater head is applied (assuming no significant changes in GW head) as the boundary condition. This is why the accumulation rate in the without-SIS scenario corresponds significantly to the river water level fluctuations.

A clear connection between the groundwater head fluctuation and the water accumulation rate can be seen. Increase of accumulation rate correlates with an increase in groundwater head. In this scenario, it seems that the groundwater head fluctuation is the main driver rather than river water level changes. In other words, when the SIS production wells are in operation, groundwater heads decline due to extraction that leads to negative accumulation rate. But, when the SIS production wells stops working (no extraction), the groundwater heads increase as the floodplain aquifer is recharged by the river and the highland groundwater. This makes the accumulation rate positive. Another explanation for this process can be a change of floodplain groundwater regime from losing (due to groundwater extraction through SIS production wells) to gaining (due to groundwater recharge). This shows that the river water level fluctuation is not the dominant driver in this situation; otherwise, an increase of accumulation rate would

NHESSD
1, 3577–3624, 2013

have occurred during the operation of the SIS production wells when the floodplain aquifer was in a losing regime.

Figure 9 shows that the amount of water moved from the river to the floodplain aquifer during the study period for the defined scenarios. Itis clearly related to the river water level. In other words, the amount of water that moves from the river to the floodplain aquifer increases with increasing river water levels and vice versa. This shows that for the study site there is a good connection between the river and the floodplain aquifer through bank recharge. On the other hand, the general trend in both scenarios is almost the same, although the amount of fluxfrom the river to the floodplain aquifer is relatively higher for the with-SIS scenario. This is attributed to the operation of the SIS production wells that creates a groundwater gradient away from the river. In the with-SIS case, fresh river water is drawn towards the SIS production wells which may result in a relatively fresher floodplain aquifer. It is worth noting that in high river level condition, as occurred at the end of the study period, less difference in the flux is observed. This means in high flow situations amount of flux is too high that groundwater extraction (at least in this scale) can make any significant difference. Also, when the SIS was shut down from November 2006 to May 2007, the flux from the river to the floodplain was same.

Following SIS commencement in July 2005, a water-table gradient away from the river developed with observation well BO3 being up to 0.5 m below the observed river level. From June and November 2006, under relatively stable river levels, observations indicate a groundwater gradient away from the river between BO1 (at the riverbank) and BO3 of 0.4 m over a distance of 130 m. During the SIS shutdown from November 2006 to May 2007, groundwater levels across Transect B1 indicated a reduced gradient with BO1, BO2, and BO3 at similar elevations. Monthly means of the BO1 hydrograph indicate groundwater elevations were greater than river levels during February, March and April 2007, indicating gaining stream conditions with the B1 and SIS midpoint hydrographs above the recorded river level. Following the reinstatement of the SIS in

NHESSD
1, 3577–3624, 2013

May 2007, recorded levels of Transect B1 wells indicate the losing stream gradient was rapidly restored and maintained in the absence of further SIS stoppages.

The dynamic of the floodplain groundwater as a hydrograph and as a longitudinal profile along transects B1 and B2 are shown in Figs. 10 and 11, respectively. In Fig. 10, the impact of groundwater lowering due to the SIS production wells is much more significant at the end of the floodplain (BO3) compared to the river bank (BO1). The only times that the two defined scenarios show the same groundwater heads are when the SIS production wells stopped working (from November 2006 to May 2007). For instance, in March 2007 the groundwater head increased to the normal level (equal to the without-SIS scenario). Given the river water level fluctuations and the groundwater responses, it can be seen that in the without-SIS scenario, the river water level change is the main driver of the surface-groundwater processes. Hence, the floodplain aquifer near the river bank (BO1) is more sensitive to the river water level changes compared to further away from the river bank (BO2 and BO3). In the with-SIS scenario, it is groundwater lowering induced by the SIS production wells that has more influence on the system. Figure 11 shows three longitudinal profiles of the floodplain aquifer groundwater head. Again, areas further away from the river banks are more influenced by the SIS production wells and these influences become more significant during the SIS operation periods.

4.2 Solute mass balance

Figure 12 shows the temporal trend of the total amount of solute mass stored in the system. The without-SIS scenario leads to a more saline floodplain aquifer, and also the amount of solute mass stored in the floodplain aquifer increase with time. In contrast, the SIS production wells maintain the floodplain aquifer salinity at a relatively stable level. Except when SIS was shut down, there was an increase in stored solute mass. In fact, the SIS production wells create a fresher floodplain aquifer by drawing the fresh river water towards the saline floodplain aquifer and extracting saline groundwater at the same time. Overall, groundwater lowering through saline groundwater extraction

NHESSD
1, 3577–3624, 2013

leads to a less saline floodplain aquifer. This is consistent with the field observations of Berens et al. (2009) and Holland et al. (2009b). According to the results, total solute mass stored in the system in with-SIS scenario reduces up to 4 % (1680 ton) while without-SIS scenario shows 2 % (846 ton) increase. Depend on the scale of the model; these values can be considerable. It is worth noting that in without-SIS scenario, there is a relative decline in solute mass in the system at the end of the study period. This is due to occurrence of river high flow before the overbank flow that happened just after the study period. Hence, in that short period solute accumulation decreased and relatively less solute mass stored in the system.

Unsaturated zone may act as an essential compartment of the solute mass stored in the floodplain aquifer. Particularly, in area such as the study site that salinity is driven by increased discharge of saline groundwater and reduced leaching of salts from the soils. High rate of ET can accelerate this process. According to the results, at the last time step (1 September 2010) in with-SIS scenario around 19 % of the total solute mass is stored in the unsaturated zone. This is 16 % for without-SIS scenario for the same time step. In fact, groundwater lowering that maintains lower water-table in the floodplain aquifer, increases the ratio of unsaturated zone to saturated zone. For instance, unsaturated nodes for the with-SIS and without-SIS scenarios are 15 647 and 12 755 out of 78 624 nodes, respectively. If only unsaturated nodes at the beginning of the study period are considered, at the last time step of the model 7120 ton solute mass is stored in the without-SIS scenario while this is 6562 ton for with-SIS scenario for the in the same nodes. Hence, groundwater extraction is able to remove some amount of solute stored in the unsaturated zone. It is worth noting that this ratio can be different for different model configuration. Perhaps shallower model (recall that this model was up to 16 m depth) gives higher ratio as ratio of unsaturated zone to the total zone is higher. Figure 13 illustrates solute mass stored in the unsaturated zone for the defined scenarios. In Fig. 13a distribution of solute mass removed from the unsaturated zone is shown. It seems groundwater extraction via SIS operation removed solute mainly from middle part of the floodplain. Figure 13b shows the amount of solute mass that

NHESSD
1, 3577–3624, 2013

could be stored in the system if SIS was not installed on the floodplain. In fact, as it could be expected without groundwater extraction more solute could have stored in the floodplain aquifer. This is consistent with results shown in Fig. 12 that groundwater extraction may lead to less saline floodplain as well as less solute mass storage in the unsaturated zone.

The dynamic of groundwater salinity is demonstrated in Fig. 14. From Fig. 14, it appears that at the relatively fresh buffer zone near the river bank, the groundwater salinity is almost the same in both scenarios. Away from the river bank, towards the SIS production wells, the influence of the SIS production wells can be clearly seen. The groundwater salinity slightly increases during the study period in the without-SIS scenario while in the other scenario the ability of the SIS operation to mitigate the salinity is significant. Again, the influence is stronger in the floodplain than close to the river bank. However, in this case, groundwater extraction is not able to change the overall pattern of the salinity of the floodplain aquifer. As, even with SIS operation there is a dramatic salinity difference between river bank (less than 7000 $\mu S\,cm^{-1}$) and the floodplain salinity (above 40 000 $\mu S\,cm^{-1}$) and decrease in salinity due to SIS is in same order.

5 Conclusions

The relative impacts of groundwater lowering through saline groundwater extraction (SIS production wells) on the interactions between a river and its adjacent semi-arid floodplain have been investigated. A fully integrated physically-based numerical model was used to simulate two defined scenarios, namely with and without SIS. The numerical model was first calibrated according to the available observed data. The results showed a reasonable correlation between observed and simulated values. The model was able to effectively reproduce the surface-groundwater interactions. Then, the calibrated model was used to simulate the defined without-SIS scenario.

NHESSD
1, 3577–3624, 2013

Water balance analyse show that groundwater extraction may change the floodplain aquifer regime from losing to gaining (or at least reduce the losing rate). This happens by changing the head gradient towards the floodplain. This can lead to more river fresh water flux to the saline floodplain aquifer and a fresh water lens along the riparian vegetation at the river bank. Also, deeper water-table is observed as a result of groundwater extraction. This is more significant in the area around the production wells in the floodplain rather than further away towards the river banks. In the without-SIS scenario it is the river water fluctuations that dominate the surface-groundwater interactions while in the other scenario; the groundwater extraction is the main driver.

In term of solute balance, SIS operation gives less saline floodplain aquifer as less amount of solute stored in the system in compare with without-SIS scenario. Moreover, it was shown that groundwater extraction is able to remove some amount of solute mass from the unsaturated zone. Overall, the saline groundwater extraction from the floodplain aquifer is shown to be an effective salt interception measure. This occurs through two mechanisms; extracting some of the solute mass from the system and changing the floodplain groundwater regime from a losing to gaining one. The latter may result in more flux from the river to the floodplain aquifer. The current management of the SIS operation seems to be effective in maintaining the floodplain salinity at a stable level.

Acknowledgements. This work was supported by the SA Water Centre for Water Management and Reuse and also the Goyder Institute for Water Research. The authors would like to acknowledge the assistance and scientific support of Ian Jolly, Kate Holland and Rebecca Doble (CSIRO), VolmerBerens (DFW), and Adrian Werner, Juliette Woods, James McCallum and Dylan Irvine (Flinders University).

NHESSD

1, 3577–3624, 2013

References

Abbott, M. B., Bathurst, J. C., Cunge, J. A., O'Connell, P. E., and Rasmussen, J.: An introduction to the European Hydrological System – Système Hydrologique Europèeen, SHE, 2: Structure of a physically-based distributed modeling system, J. Hydrol., 87, 61–77, 1986.

Allison, G. B., Cook, P. G., Barnett, S. R., Walker, G. R., Jolly, I. D., and Hughes, M. W.: Land clearance and river salinization in the western Murray Basin, Australia, J. Hydrol., 119, 1–20, 1990.

Anderson, M. P. and Woessner, W. W.: Applied Groundwater Modelling: Simulation of Flow and Advective Transport, Academic Press, San Diego, USA, 1992.

AquaVeo: GMS, Provo, Utah, United States, 2011.

Banks, E. W., Brunner, P., and Simmons, C. T.: Vegetation controls on variably saturated processes between surface water and groundwater and their impact on the state of connection, Water Resour. Res., 47, W11517, doi:10.1029/2011WR010544, 2011.

Barnett, B., Townley, L. R., Post, V., Evans, R. E., Hunt, R. J., Peeters, L., Richardson, S., Werner, A. D., Knapton, A., and Boronkay, A.: Australian groundwater modelling guidelines, National Water Commission, Canberra, 2012.

Berens, V., White, M., and Souter, N.: Bookpurnong Living Murray Pilot Project: a trial of three floodplain water management techniques to improve vegetation condition, Department of Water, Land and Biodiversity Conservation, Adelaide, 2009.

Beven, K.: On explanatory depth and predictive power, Hydrol. Process., 15, 3069–3072, 2001.

Beven, K.: Towards a coherent philosophy for modelling the environment, P. Roy. Soc. Lond. A Mat., 458, 2465–2484, 2002.

Beven, K.: A manifesto for the equifinality thesis, J. Hydrol., 320, 18–36, 2006.

Beven, K. and Binley, A.: The future of distributed models: model calibration and uncertainty prediction, Hydrol. Process., 6, 279–298, 1992.

Brooks, R. J. and Corey, A. T.: Hydraulic properties of porous media, in: Hydrology Paper No. 3, Colorado State University, Fort Collins, 1964.

Brown, C. M. and Stephenson, A. E.: Geology of the Murray Basin, Southeastern, Bureau of Mineral Resources Bulletin, 235 pp., 1991.

Brunner, P. and Simmons, C. T.: HydroGeoSphere: a fully integrated, physically based hydrological model, Ground Water, 50, 170–176, 2012.

NHESSD
1, 3577–3624, 2013

Brutsaert, W. and Lopez, J. P.: Basin-scale geohydrologic drought flow features of riparian aquifers in the southern Great Plains, Water Resour. Res., 34, 233–240, 1998.
Camporese, M., Paniconi, C., Putti, M., and Orlandini, S.: Surface-subsurface flow modeling with path-based runoff routing, boundary condition-based coupling, and assimilation of multisource observation data, Water Resour. Res., 46, W02512, doi:10.1029/2008WR007536, 2010.
Chen, X.: Stream water infiltration, bank storage, and storage zone changes due to stream-stage fluctuations, J. Hydrol., 280, 246–264, 2003.
Chen, X. and Shu, L.: Groundwater evapotranspiration captured by seasonally pumped wells in river valleys, J. Hydrol., 318, 334–347, 2006.
Doble, R.: Quantifying spatial distributions of groundwater discharge and salt accumulation on a semi-arid floodplain to determine vegetation health response, Ph.D. thesis, School of Chemistry, Physics and Earth Sciences, Flinders University of South Australia, Adelaide, 371 pp., 2004.
Doble, R., Simmons, C., Jolly, I., and Walker, G.: Spatial relationships between vegetation cover and irrigation-induced groundwater discharge on a semi-arid floodplain, Australia, J. Hydrol., 329, 75–97, doi:10.1016/j.jhydrol.2006.02.007, 2006.
DWR: South Australian River Murray Salinity Strategy 2001–2015, Department for Water Resources, Government of South Australia, Adelaide, 2001.
Ebel, B. A. and Loague, K.: Physics-based hydrologic-response simulation: seeing through the fog of equifinality, Hydrol. Process., 20, 2887–2900, 2006.
Franke, O. L., Reily, T. E., and Bennett, G. D.: Definition of boundary and initial conditions in the anaysis of saturated ground-water flow systems; an introduction, USGS, Book 3, Chapter B5, 15 pp., 1987.
Freeze, R. A. and Harlan, R. L.: Blueprint for a physically-based, digitally-simulated hydrologic response model, J. Hydrol., 9, 237–258, 1969.
Hart, B., Bailey, P., Edwards, R., Hortle, K., James, K., McMahon, A., Meredith, C., and Swadling, K.: A review of the salt sensitivity of the Australian freshwater biota, Hydrobiologia, 210, 105–144, 1991.
Herczeg, A. L., Simpson, H. J., and Mazor, E.: Transport of soluble salts in a large semiarid basin: River Murray, Australia, J. Hydrol., 144, 59–84, 1993.
Hingston, F. J., Galbraith, J. H., and Dimmock, G. M.: Application of the process-based model BIOMASS to Eucalyptus globules subsp. Globules plantations on ex-farmland in south

NHESSD
1, 3577–3624, 2013

Western Australia: I. Water use by trees and assessing risk of losses due to drought, Forest Ecol. Manag., 106, 141–156, 1997.
Hoehn, E. and Scholtis, A.: Exchange between a river and groundwater, assessed with hydrochemical data, Hydrol. Earth Syst. Sci., 15, 983–988, doi:10.5194/hess-15-983-2011, 2011.
Holland, K. L., Jolly, I. D., Overton, I. C., and Walker, G. R.: Analytical model of salinity risk from groundwater discharge in semi-arid, lowland floodplains, Hydrol. Process., 23, 3428–3439, 2009a.
Holland, K. L., Doody, M. T., McEwan, K. L., Jolly, I. D., White, M., Berens, V., and Souter, N.: Response of the River Murray floodplain to flooding and groundwater management: field investigations, CSIRO, 65 pp., 2009b.
Holland, K. L., Doody, T. M., McEwan, K. L., Jolly, I. D., White, M., Berens, V., and Souter, N. J.: Response of the River Murray floodplain to flooding and groundwater management: field investigations, CSIRO, Adelaide, Australia, 65 pp., 2009c.
HydroGeoLogic Inc: MODHMS: a comprehensive MODFLOW-based hydrologic modelling system, version 3.0, HydroGeoLogic Incorporated, Herndon, USA, 2006.
Jarwal, S. D., Walker, G. R., and Jolly, I. D.,: General site description; Salt and Water Movement in the Chowilla Floodplain, CSIRO Division of Water Resources, Canberra, Australia, 16–309, 1996.
Jolly, I. D., Walker, G. R., and Thorburn, P. J.: Salt accumulation in semi-arid floodplain soils with implications for forest health, J. Hydrol., 150, 589–614, doi:10.1016/0022-1694(93)90127-u, 1993.
Jolly, I. D., Walker, G. R., Hollingworth, I. D., Eldridge, S. R., Thorburn, P. J., McEwan, K. L., and Hatton, T. J.: The causes of decline in eucalypt communities and possible ameliorative approaches, in: Salt and Water Movement in the Chowilla Floodplain, edited by: Walker, G. R., Jolly, I. D., and Jarwal, S. D., CSIRO Division of Water Resources, Canberra, Australia, 23–45 1996.
Jolly, I. D., McEwan, K. L., and Holland, K. L.: A review of groundwater-surface water interactions in arid/semi-arid wetlands and the consequences of salinity for wetland ecology, Ecohydrology, 1, 43–58, 2008.
Kollet, S. J. and Maxwell, R. M.: Integrated surface-groundwater flow modeling: a free-surface overland flow boundary condition in a parallel groundwater flow model, Adv. Water Resour., 29, 945–958, doi:10.1016/j.advwatres.2005.08.006, 2006.

NHESSD
1, 3577–3624, 2013

Krause, S., Bronstert, A., and Zehe, E.: Groundwater-surface water interactions in a North German lowland floodplain – implications for the river discharge dynamics and riparian water balance, J. Hydrol., 347, 404–417, doi:10.1016/j.jhydrol.2007.09.028, 2007.
Kristensen, K. J. and Jensen, S. E.: A model for estimating actual evapotranspiration from potential evapotranspiration, Nord. Hydrol., 6, 170–188, doi:10.2166/nh.1975.012, 1975.
Lamontagne, S., Leaney, F. W., and Herczeg, A. L.: Groundwater–surface water interactions in a large semi-arid floodplain: implications for salinity management, Hydrol. Process., 19, 3063–3080, 2005.
Leavesley, G. H., Restrepo, P. J., Markstrom, S. L., Dixon, M., and Stannard, L. G.: The modular modeling system (MMS): User's manual, USGS, Reston, Virginia, 1996.
Lenahan, M. J. and Bristow, K. L.: Understanding sub-surface solute distributions and salinization mechanisms in a tropical coastal floodplain groundwater system, J. Hydrol., 390, 131–142, doi:10.1016/j.jhydrol.2010.06.009, 2010.
Li, Q., Unger, A. J. A., Sudicky, E. A., Kassenaar, D., Wexler, E. J., and Shikaze, S.: Simulating the multi-seasonal response of a large-scale watershed with a 3-D physically-based hydrologic model, J. Hydrol., 357, 317–336, 2008.
Liang, D., Falconer, R., and Lin, B.: Coupling surface and subsurface flow in a depth averaged flood wave model, J. Hydrol., 337, 147–158, 2007.
Loague, K. and VanderKwaak, J. E.: Physics-based hydrologic response simulation: platinum bridge, 1958 Edsel, or useful tool?, Hydrol. Process., 16, 1015–1032, 2004.
McLaren, R. G.: Grid Builder: a pre-processor for 2-D, triangular element, finite-element programs, Groundwater Simulations Group, GRIDBUILDER user manual, University of Waterloo, Waterloo, Ontario, 2005.
MDBA: Report of the Independent Audit Group for Salinity 2008–2009, Murray–Darling Basin Authority (MDBA), Canberra, Australia, 2010.
Meire, D., De Doncker, L., Declercq, F., Buis, K., Troch, P., and Verhoeven, R.: Modelling river-floodplain interaction during flood propagation, Nat. Hazards, 55, 111–121, 2010.
Moench, A. F. and Barlow, P. M.: Aquifer response to stream-stage and recharge variations, I. Analytical step-response functions, J. Hydrol., 230, 192–210, 2000.
Nasonova, O. and Gusev, E.: Investigating the ability of a land surface model to reproduce river runoff with the accuracy of hydrological models, Water Resour., 35, 493–501, doi:10.1134/s0097807808050011, 2008.

NHESSD
1, 3577–3624, 2013

Overton, I. and Jolly, I.: Integrated Studies of Floodplain Vegetation Health, Saline Groundwater and Flooding on the Chowilla Floodplain South Australia, Adelaide, Australia, CSIRO, 2004.
Panday, S. and Huyakorn, P.: A fully coupled physically-based spatially-distributed model for evaluating surface/subsurface flow, Adv. Water Resour., 27, 361–382, 2004.
Peck, A. J. and Hatton, T.: Salinity and the discharge of salts from catchments in Australia, J. Hydrol., 272, 191–202, 2003.
Peck, A. J. and Hurle, D. H.: Chloride balance of some farmed and forested catchments in Southwestern Australia, Water Resour. Res., 9, 648–657, 1973.
Petheram, C., Bristow, K. L., and Nelson, P. N.: Understanding and managing groundwater and salinity in a tropical conjunctive water use irrigation district, Agr. Water Manage., 95, 1167–1179, 2008.
Pilgrim, D. H., Chapman, T. G., and Doran, D. G.: Problems of rainfall runoff modelling in arid and semi-arid regions, Hydrolog. Sci. J., 33, 379–400, 1988.
Qu, Y. and Duffy, C. J.: A semidiscrete finite volume formulation for multiprocess watershed simulation, Water Resour. Res., 43, W08419, doi:10.1029/2006WR005752, 2007.
Rassam, D. W.: A conceptual framework for incorporating surface-groundwater interactions into a river operation-planning model, Environ. Modell. Softw., 26, 1554–1567, 2011.
Ross, M. A., Tara, P. D., Geurink, J. S., and Stewart, M. T.: FIPR hydrologic model users' manual and technical documentation, University of South Florida, Tampa, 1997.
Shlychkov, V.: Numerical modeling of river flows with account for vortex generation at the channel-floodplain boundary, Water Resour., 35, 522–529, doi:10.1134/s0097807808050035, 2008.
Sophocleous, M.: Review: Groundwater management practices, challenges, and innovations in the High Plains aquifer, USA – lessons and recommended actions, Hydrogeol. J., 18, 559–575, doi:10.1007/s10040-009-0540-1, 2010.
Sophocleous, M. S. and Perkins, P.: Methodology and application of combined watershed and ground-water models in Kansas, J. Hydrol., 236, 185–201, 2000.
Sophocleous, M., Koussis, A., Martin, J. L., and Perkins, S. P.: Evaluation of simplified stream-aquifer depletion models for water rights administration, Ground Water, 33, 579–588, 1995.
Squillace, P. J.: Observed and simulated movement of bank-storage water, Ground Water, 34, 121–134, 1996.
Sun, D. and Zhan, H.: Pumping induced depletion from two streams, Adv. Water Resour., 30, 1016–1026, 2007.

NHESSD
1, 3577–3624, 2013

Therrien, R.: Three-dimensional analysis of variablysaturated flow and solute transport in discretely-fractured porous media, Ph.D. thesis, University of Waterloo, Waterloo, Canada, 1992.

Therrien, R. and Sudicky, E. A.: Three-dimensional analysis of variably-saturated flow and solute transport in discretely-fractured porous media, J. Contam. Hydrol., 23, 1–44, 1996.

Therrien, R., McLaren, R. G., Sudicky, E. A., and Panday, S. M.: HydroGeoSphere: a Three-Dimensional Numerical Model Describing Fully-Integrated Subsurface and Surface Flow and Solute Transport, Groundwater Simulations Group, University of Waterloo, Waterloo, Canada, 2005.

Therrien, R., McLaren, R. G., Sudicky, E. A., and Panday, S. M.: HydroGeoSphere: a Three-dimensional Numerical Model Describing Fully-integrated Subsurface and Surface Flow and Solute Transport, Groundwater Simulations Group, University of Waterloo, Waterloo, Canada, 2010a.

Therrien, R., McLaren, R. G., Sudicky, E. A., and Panday, S. M.: HydroGeoSphere: a Three-dimensional Numerical Model Describing Fully-integrated Subsurface and Surface Flow and Solute Transport: User Manual, Groundwater Simulations Group, University of Waterloo, Waterloo, Ontario, Canada, 2010b.

van Genuchten, M. T.: A closed-form equation for predicting the hydraulic conductivity of unsaturated soils, Soil Sci. Soc. Am. J., 44, 892–898, 1980.

VanderKwaak, J. E.: Numerical simulation of flow and chemical transport in integrated surface-subsurface hydrologic systems, Ph.D. thesis, University of Waterloo, Waterloo, Canada, 1999.

VanderKwaak, J. E. and Loague, K.: Hydrologic-response simulations for the R-5 catchment with a comprehensive physics-based model, Water Resour. Res., 37, 999–1013, 2001.

Verstrepen, L.: Evaluating rainwater harvesting on watershed level in the semi-arid zone of Chile, M.Sc. thesis, Bioscience Engineering, Universiteit Gent, Gent, 113 pp., 2011.

Viezzoli, A., Auken, E., and Munday, T.: Spatially constrained inversion for quasi 3-D modelling of airborne electromagnetic data – an application for environmental assessment in the Lower Murray Region of South Australia, Explor. Geophys., 40, 173–183, doi:10.1071/EG08027, 2009.

Wheater, H. S., Mathias, S. A., and Li, X.: Groundwater Modelling in Arid and Semi-Arid Areas, Cambridge University Press, Cambridge, 2010.

NHESSD

1, 3577–3624, 2013

White, M. G., Berens, V., and Souter, N. J.: Bookpurnong Living Murray Pilot Project: artificial inundation of *Eucalyptus camaldulensis* on a floodplain to improve vegetation condition, Science, Monitoring and Information Division, Department of Water, Land and Biodiversity Conservation, Adelaide, Australia, 2009.

Winter, T. C.: Relation of streams, lakes, and wetlands to groundwater flow systems, Hydrogeol. J., 7, 28–45, doi:10.1007/s100400050178, 1999.

NHESSD

1, 3577–3624, 2013

Table 1. Porous media and van Genuchten function parameter values.

	k isotropic (md^{-1})	Specific storage (m^{-1})	Transverse dispersivity (m)	Longitudinal dispersivity (m)	Porosity ($m^3 m^{-3}$)	van Genuchten functions parameters		
						Alpha (m^{-1})	Beta (dimensionless)	Residual saturation
Clay	0.1	0.002	0.5	5	0.6	0.28	2.52	0.0
Sand	10	0.00016	0.5	5	0.35	1.69	8.25	0.03

NHESSD
1, 3577–3624, 2013

Table 2. Surface properties values of the numerical model.

	x friction	y friction	Rill storage height (m)	Obstruction storage height (m)	Coupling length (m)	Longitudinal dispersivity (m)	Transverse dispersivity (m)
River	0.005	0.005	0.0001	0	0.01	1	1
Floodplain	0.05	0.05	0.01	0	0.01	1	1

NHESSD
1, 3577–3624, 2013

Table 3. ET component parameters values for the study site.

	Eucalyptus	Grass
Canopy storage parameter (m)	0.00045	0.04
Initial interception storage (m)	0.0003	0.04
Transpiration fitting		
C1	0.3	0.6
C2	0.2	0
C3	1	1
Transpiration limiting saturations		
wilting point	0.29	0.29
field capacity	0.56	0.56
oxic limit	0.85	0.75
anoxic limit	0.95	0.9
Evaporation limiting saturations	0.22	0.25
	0.95	0.9
LAI	1.5	0.5
Root depth (m)	5	0.5
Evaporation depth (m)	1	1

NHESSD
1, 3577–3624, 2013

Table 4. Results of the calibrated model performance statistics.

Observation Wells	R^2	N_r	MSR (m)	RMSE (m)
BO1	0.91	0.76	0.054	0.067
BO2	0.87	0.71	0.075	0.088
BO3	0.85	0.657	0.080	0.091
BO4	0.83	0.77	0.044	0.058
BO5	0.83	0.63	0.031	0.041
BO6	0.81	0.61	0.048	0.061

NHESSD
1, 3577–3624, 2013

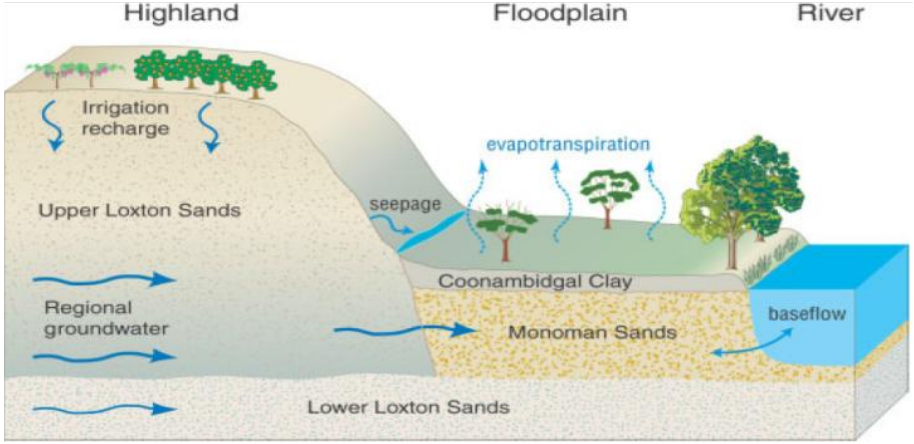

Fig. 1. Conceptual model of groundwater inputs to the floodplain and potential groundwater discharge pathways within the floodplain in the Lower River Murray (Holland et al., 2009a).

NHESSD
1, 3577–3624, 2013

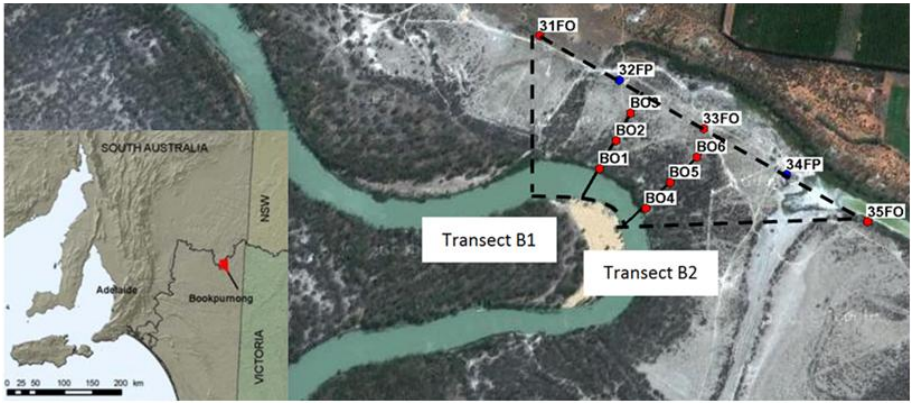

Fig. 2. Configuration of SIS production wells (in blue) and observation wells (in red) at the Clark's Floodplain. The inset map shows the location of the Bookpurnong floodplain in the South Australian.

NHESSD
1, 3577–3624, 2013

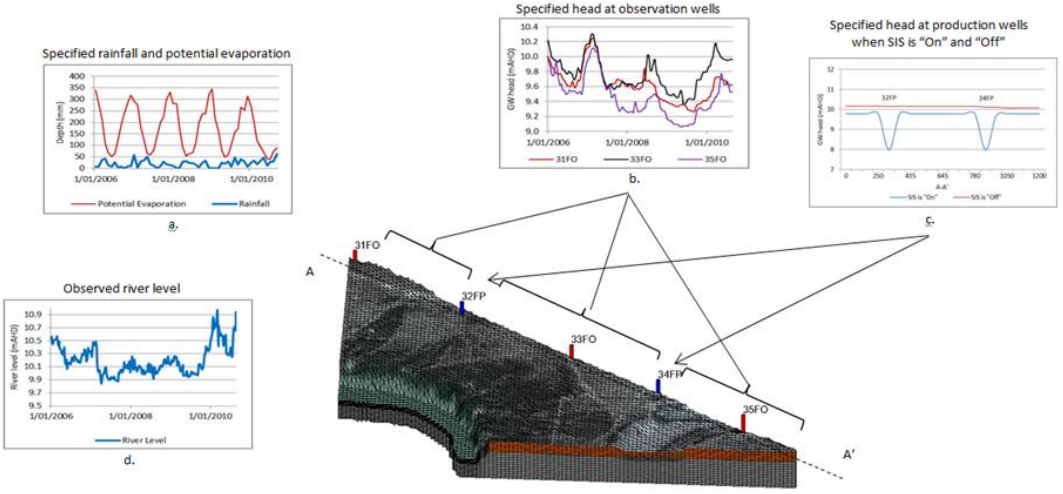

Fig. 3. Configuration of boundary conditions for river, floodplain and groundwater domains. Soil layers consist of Coonambidgal Clay in orange and Monoman Sand in grey.

NHESSD
1, 3577–3624, 2013

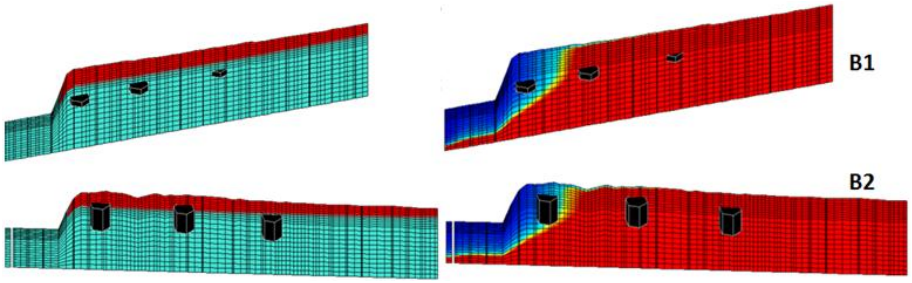

Fig. 4. 3-D demonstration of simulated initial condition along transects B1 and B2: **(a)** porous media saturation. (Saturated zone is shown in light blue and unsaturated in red.) **(b)** Solute concentration distribution (salinity above 7000 $\mu S\,cm^{-1}$ in red and less than 7000 $\mu S\,cm^{-1}$ in blue). Observation wells are in black.

NHESSD
1, 3577–3624, 2013

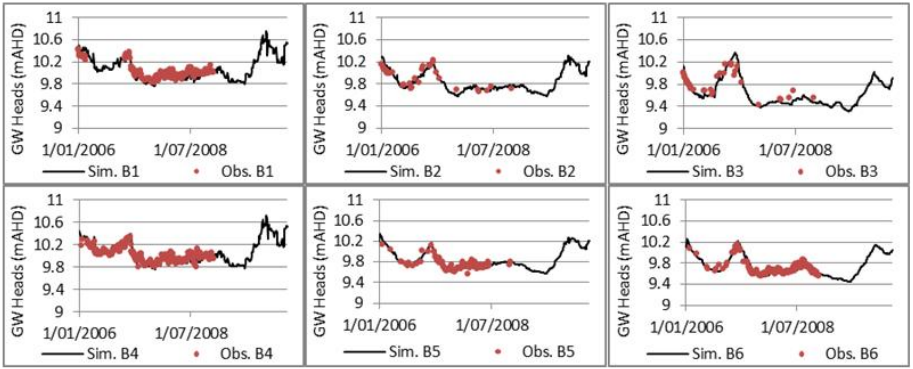

Fig. 5. Simulated and observed groundwater heads at observation wells.

NHESSD
1, 3577–3624, 2013

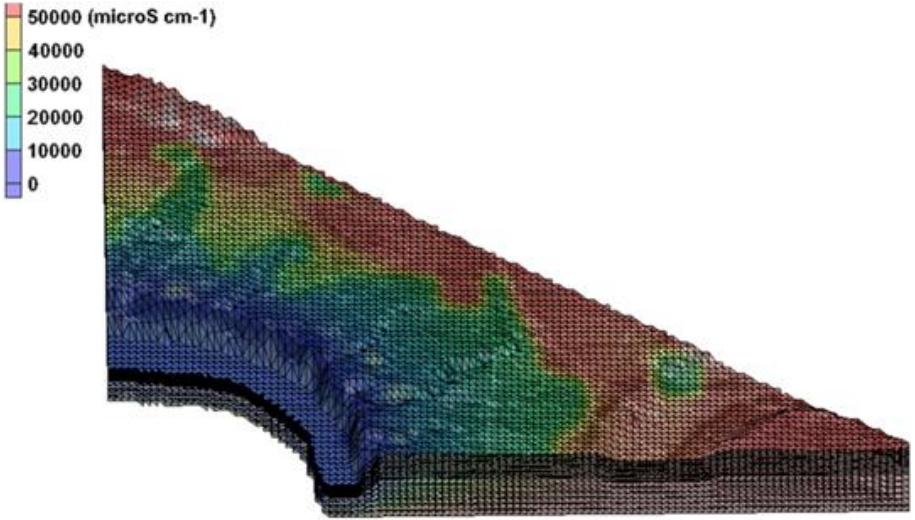

Fig. 6. 3-D visualization of the solute distribution for the calibration model snapshot of the last day of the simulation (1 September 2010).

NHESSD
1, 3577–3624, 2013

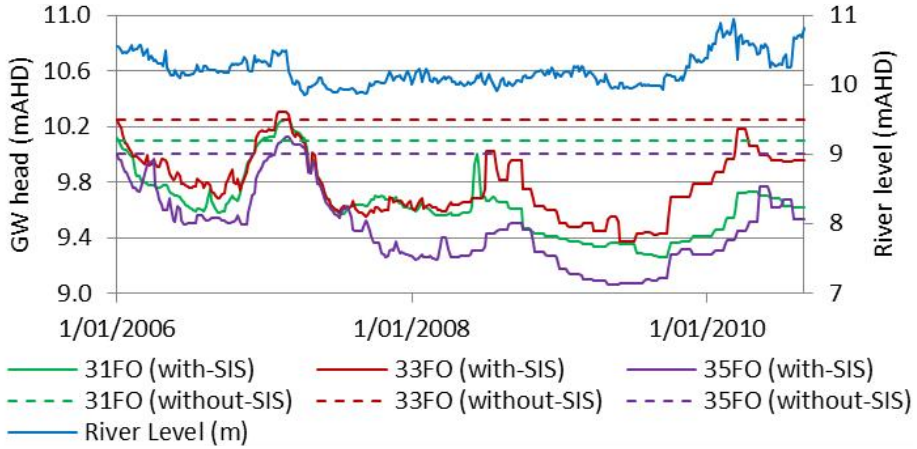

Fig. 7. Groundwater heads at the boundary of the models (SIS wells) for the defined scenarios.

NHESSD
1, 3577–3624, 2013

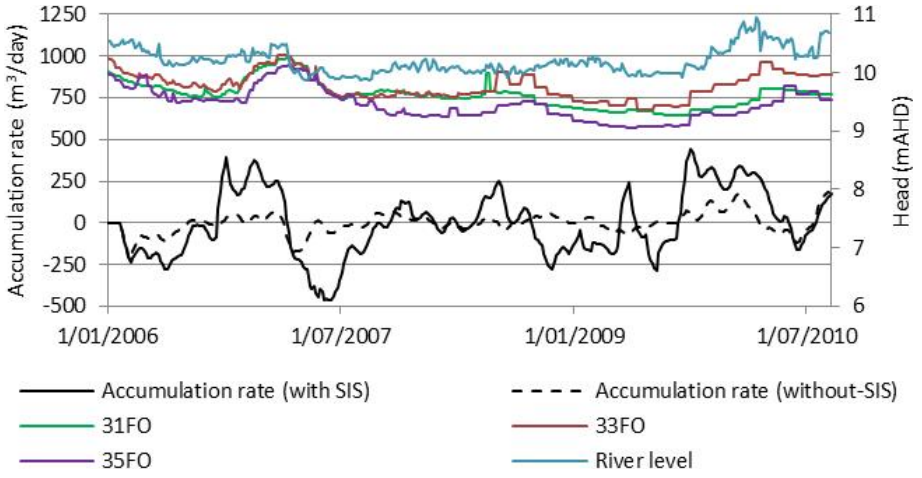

Fig. 8. Results of water accumulation rates in the porous media for the defined scenarios.

NHESSD
1, 3577–3624, 2013

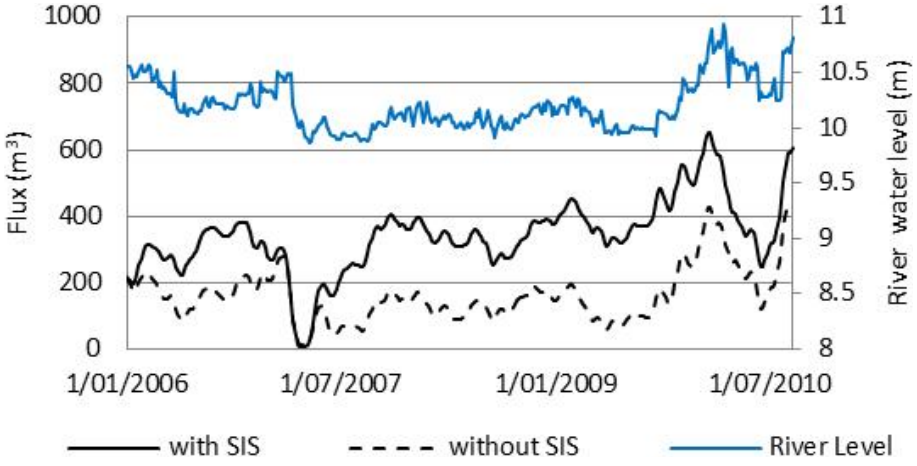

Fig. 9. Results of water flux from the river to the floodplain aquifer for the defined scenarios.

NHESSD
1, 3577–3624, 2013

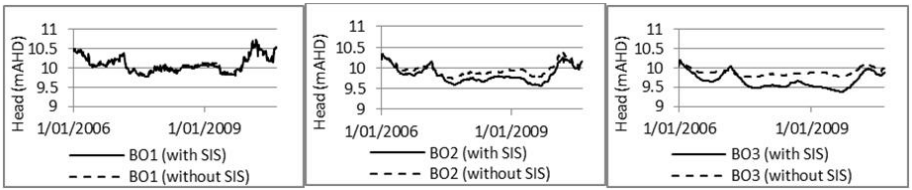

Fig. 10. GW head dynamics at the observation wells on transect B1 for the with-SIS and without-SIS scenarios.

NHESSD
1, 3577–3624, 2013

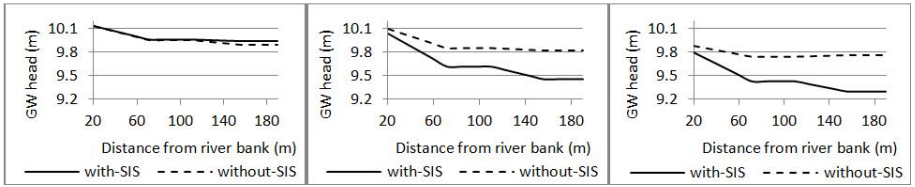

Fig. 11. GW head longitudinal profiles on 7 March 2007 (left), 16 December 2008 (middle) and 29 July 2009 (right) on transect B2 for the with-SIS and without-SIS scenarios.

NHESSD
1, 3577–3624, 2013

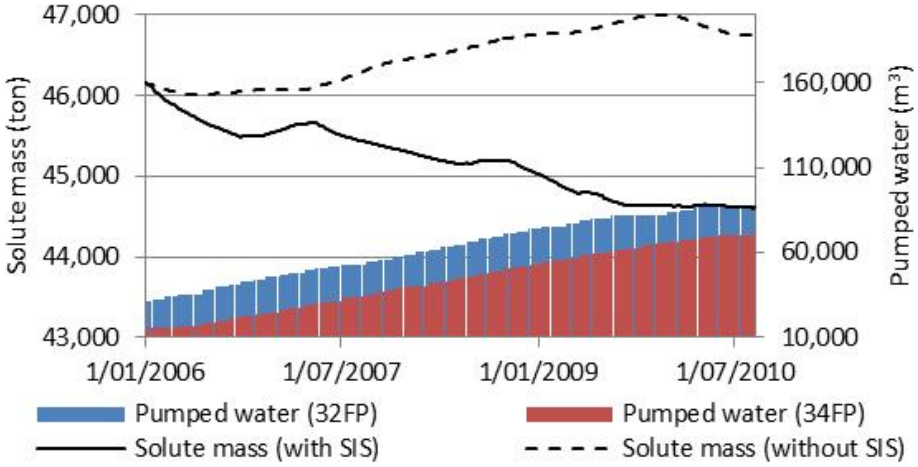

Fig. 12. Total solute mass stored in the system in each time step for the defined scenarios. Cumulative pumped water is also shown.

NHESSD
1, 3577–3624, 2013

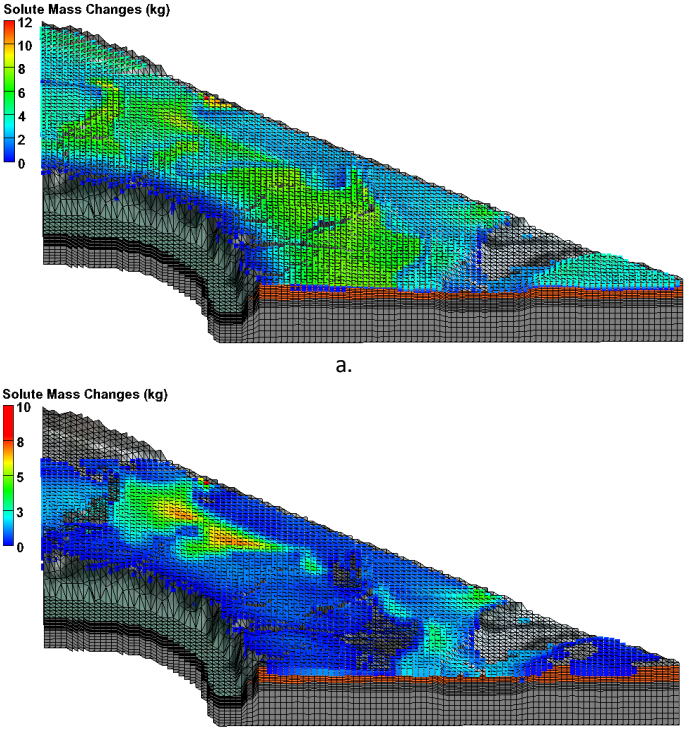

Fig. 13. 3-D visualization of solute mass stored in the unsaturated zone for the defined scenarios; **(a)** amount of solute mass removed from the unsaturated zone during the with-SIS scenario, **(b)** amount of solute mass that could be stored in the system if SIS was not installed on the floodplain.

NHESSD
1, 3577–3624, 2013

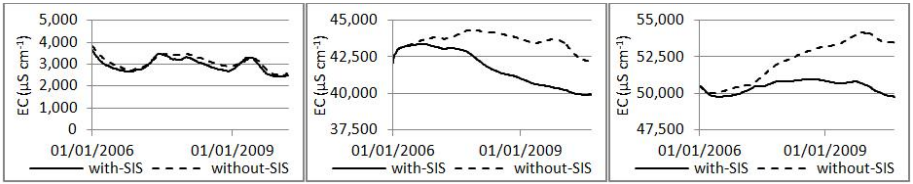

Fig. 14. Solute dynamics at the observation wells BO1 (left), BO2 (middle) and BO3 (right).

NHESSD
1, 3577–3624, 2013